

- Compromising Differentiation Potential. *Gene Therapy* 18:857-866, 2011.
2. Miyake K, Hirasawa T, Soutome M, Itoh M, O Goto Y, Endoh K, Takahashi K, Kudo S, Nakagawa T, Yokoi S, Taira T, Inazawa J, Kubota T. The protocadherins, PCDHB1 and PCDH7, are regulated by MeCP2 in neuronal cells and brain tissues: implication for pathogenesis of Rett syndrome. *BMC Neuroscience* 12:81, 2011
 3. Waga C, Okamoto N, Ondo Y, Fukumura-Kato R, O Goto Y, Kohsaka S, Uchino S. Novel variants of the SHANK3 gene in Japanese autistic patients with severe delayed speech development. *Psychiatr Genet* 21:208-11, 2011
 4. Takeshita E, Saito Y, Nakagawa E, Komaki H, Sugai K, Sasaki M, Nezu A, Kitamura J, Itoh M, Sawano Y, O Goto Y. Late-onset mental deterioration and fluctuating dystonia in a female patient with a truncating MECP2 mutation. *J Neurol Sci* 308:168-72, 2011

研究分担者：功刀浩

1. Sasayama D, Hori H, Teraishi T, Hattori K, Ota M, Matsuo J, Kawamoto Y, Kinoshita Y, Hashikura M, Amano N, Higuchi T, O Kunugi H. More severe impairment of manual dexterity in bipolar disorder compared to unipolar major depression. *J Affect Disord*. 2012 Feb;136(3):1047-52. Epub 2011 Dec 12. PubMed PMID: 22169250.
2. Wakabayashi C, Numakawa T, Ninomiya M, Chiba S, O Kunugi H. Behavioral and molecular evidence for psychotropic effects in L: -theanine. *Psychopharmacology (Berl)*. 2012 Feb;219(4):1099-109. Epub 2011 Aug 23. PubMed PMID: 21861094.
3. O 功刀 浩：ドパミン受容体作動薬とうつ病。内分泌・糖尿病・代謝内科（印刷中）

研究分担者：川寄弘詔

1. Takata A, O Kawasaki H, Iwayama Y, Yamada K, Gotoh L, Mitsuyasu H, Miura T, Kato T, Yoshikawa T, Kanba S: Nominal association between a polymorphism in DGKH and bipolar disorder detected in a meta-analysis of East Asian case-control samples. *Psychiatry Clin Neurosci*, 65(3):280-5, 2011
2. 尾崎紀夫, 坂本薫, O 川寄弘詔, 加藤正木: 双極性障害における新たな治療選択肢 -Lamotrigine の適応拡大を前に-. *臨床精神薬理*, 14(9): 1567-1575, 2011
3. O 川寄弘詔: 院内における中立性を担保する第三者としての精神科医は、いかにドナー候補の同意能力および自発意識を評価するのか. *今日の移植*, 24(2): 141-146, 2011
4. O 川寄弘詔, 光安博志: 双極 I 型障害と双極 II 型障害の違いを教えてください. うつ病の事典～うつ病と双極性障害がわかる本 (樋口輝彦, 野村総一郎, 加藤忠史編著), 第 9 章 双極性障害のさまざまなタイプ, (神庭重信監修), pp84-86, こころの科学特別号, 日本評論社, 東京, 2011
5. O 川寄弘詔: 院内における中立性を担保する第三者としての精神科医は、いかにドナ

- 一候補の同意能力および自発意識を評価するのか. 移植, 46(1): 18-26, 2011
6. 春木繁一, 西村勝治, 阿部祥, 梅谷由美, 南里幸一郎, 桂川修一, 小林清香, 川岸直樹, 菅原寧彦, ○川寄弘詔: 討論: 特集 1 第 46 回日本移植学会ワークショップ “生体ドナーの意思決定にどのようにかかわるか”. 今日の移植, 24(2): 161-164, 2011
 7. ○川寄弘詔: 双極スペクトラムを巡って「第 107 回日本精神神経学会学術総会」より. 月刊 JMS 12 月号, pp42-45, 株式会社ジャパンメディカルソサエティ, 東京, 2011
 8. ○川寄弘詔: STEP-BD. リンケージ解析 [連鎖解析]. 現代精神医学事典 (加藤敏, 神庭重信, 中谷陽二, 武田雅俊, 鹿島晴雄, 狩野力八郎, 市川宏伸編), p564, p1072, 弘文社, 東京, 2011

研究分担者：米本直裕

1. Matsuoka Y, Nishi D, ○Yonemoto N, Hamazaki K, Hamazaki T, Hashimoto K.(2011) Potential role of brain-derived neurotrophic factor in omega-3 Fatty Acid supplementation to prevent posttraumatic distress after accidental injury: an open-label pilot study. *Psychother Psychosom*, 80(5), 310-2.
2. Furukawa TA, Akechi T, Shimodera S, Yamada M, Miki K, Watanabe N, Inagaki M, ○Yonemoto N.(2011) Strategic use of new generation antidepressants for depression: SUN(^_^)D study protocol. *Trials*. 11;12:116.
3. Nagai S, ○Yonemoto N, Rabesandratana N, Andrianarimanana D, Nakayama T, Mori R.(2011) Long-term effects of earlier initiated continuous Kangaroo Mother Care (KMC) for low-birth-weight (LBW) infants in Madagascar. *Acta Paediatr*. 100(12):e241-7.
4. 山田光彦, 稲垣正俊, ○米本直裕 (2011) 向精神薬と自殺予防, 臨床精神薬理 第 14 巻 12 号

研究分担者：玉浦明美

研究分担者：松岡豊

1. Komachi M, Kamibeppu K, Nishi D, ○Matsuoka Y: Secondary traumatic stress and associated factors among Japanese nurses working in hospitals. *Int J Nurs Practice* (in press)
2. Nishi D, Usuki M, Matsuoka Y: Peritraumatic distress in accident survivors: An indicator for posttraumatic stress, depressive and anxiety symptoms, and posttraumatic growth. In *Post Traumatic Stress Disorders*, InTech Open Access Publisher, Croatia, pp97-112, 2011 [ISBN 978-953-307-825-0]
3. Matsumura K, Noguchi H, Nishi D, ○Matsuoka Y: Effect of omega-3 fatty acids on the psychological assessment for secondary prevention of posttraumatic stress disorder: an open-label pilot study. *Global J Health Science* 4(1): 3-9, 2012

4. ○Matsuoka Y, Nishi D, Nakaya N, Sone T, Hamazaki K, Hamazaki T, Koido Y: Attenuating posttraumatic distress with omega-3 polyunsaturated fatty acids among disaster medical assistance team members after the Great East Japan Earthquake: The APOP randomized controlled trial. *BMC Psychiatry* 2011 Aug 16;11:132
5. ○Matsuoka Y, Nishi D, Yonemoto N, Hamazaki K, Hamazaki T, Hashimoto K: Potential role of brain-derived neurotrophic factor in omega-3 fatty acid supplementation to prevent posttraumatic distress after accidental injury: An open-label pilot study. *Psychother Psychosom* 2011;80:310-312
6. ○松岡豊, 西大輔: 魚油による PTSD 予防への挑戦. *精神神経学雑誌* 114:2012 (印刷中)
7. 臼杵正人, ○松岡豊, 西大輔: 集中治療室における急性ストレス障害 (ASD) と心的外傷後ストレス障害 (PTSD). *救急医療*, 2012 (印刷中)
8. 臼杵正人, 西大輔, ○松岡豊: 急性ストレス反応 (ASD)、心的外傷後ストレス障害 (PTSD) 患者への対応について教えてください. *救急・集中医療* 24(1-2), 2012 (印刷中)
9. 西大輔, ○松岡豊: オメガ 3 系脂肪酸の可能性—うつ病および PTSD の治療と予防に向けて. *食品と開発* 47 (2): 25-27, 2012
10. 西大輔, 臼杵正人, 松村健太, ○松岡豊: 事故後の PTSD の予防に向けて. *精神科* 18(6):659-663, 2011
11. ○松岡豊: 魚油による PTSD 予防への挑戦. *分子精神医学* 11(2): 154-156, 2011
12. ○松岡豊, 浜崎景: うつ病と ω3 系多価不飽和脂肪酸. *Depression Frontier* 9(1):35-43, 2011

研究分担者: 中川敦夫

1. ○中川敦夫: 【うつ病の評価と治療】 うつ病治療のエビデンス・アップデート—薬物療法と認知行動療法を中心に—, *日本病院薬剤師会雑誌*, 47(2): 173-175, 2011
2. ○中川敦夫: 【うつ病のお薬】 SSRI で自殺が増えたといわれますが、本当でしょうか?, *こころのりんしょう a・la・carte*, 30(1): 37, 2011
3. ○中川敦夫: 【うつ病のお薬】 抗うつ薬と自殺関連リスク, *こころのりんしょう a・la・carte*, 30(1): 105-110, 2011
4. 加藤健徳, ○中川敦夫, 須藤清美, 井川恵子, 岩下覚, 【これからの精神科地域ケア—統合失調症を中心に—】 *地域ケア時代の治療スキル 治療ガイドラインの活用*, *臨床精神医学*, 40(5): 659-665, 2011
5. ○中川敦夫: 【震災に伴う心のケア】 災害・災害関連事象に伴う不安への対応と対処—認知療法的な観点から—, *心と社会*, 42(3): 22-26, 2011
6. ○中川敦夫: 【内科医のためのうつ病診療—一般内科医の対処と診療のすべて】 *治療/実地医家が可能なうつ病診療の実際—うつ病の認知療法・認知行動療法の実際*, *Medical Practice*, 28(10): 1846-1850, 2011
7. Ono Y, Furukawa TA, Shimizu E, Okamoto Y, ○Nakagawa A, Fujisawa D, Ishii T, Nakajima

- S., Current status of research on cognitive therapy/cognitive behavior therapy in Japan. *Psychiatry Clin Neurosci* 2011 Mar;65(2):121-129.
8. Fujisawa, D., Nakagawa, A., Kikuchi, T., Sado, M., Tajima, M., Hanaoka, M., Wright, J.H., Ono, Y., 2011. Reliability and validity of the Japanese version of the Cognitive Therapy Awareness Scale: a scale to measure competencies in cognitive therapy. *Psychiatry Clin Neurosci* 2011 Feb;65(1): 64-69.
 9. Brian S. Everitt, Simon Wessley(著), 樋口輝彦, 山田光彦(監訳), 中川敦夫, 米本直裕(訳) ロンドン大学精神医学研究所に学ぶ 精神科臨床試験の実践, 2011. 医学書院, 東京.

研究分担者：橋本亮太

1. Takahashi H, Iwase M, Yasuda Y, Ohi Y, Fukumoto M, Iike N, Yamamori H, Nakahachi T, Ikezawa K, Azechi M, Canuet L, Ishii R, Kazui H, Hashimoto R, Takeda M. Relationship of Prepulse Inhibition to Temperament and Character in Healthy Japanese subjects. *Neuroscience Research* (in press)
2. Ohi K, Hashimoto R, Yasuda Y, Fukumoto M, Nemoto K, Ohnishi T, Yamamori H, Takahashi H, Iike N, Kamino K, Yoshida T, Azechi M, Ikezawa K, Tanimukai H, Tagami S, Morihara T, Okochi M, Tanaka T, Kudo T, Iwase M, Kazui H, Takeda M. The AKT1 gene is associated with attention and brain morphology in schizophrenia. *World J Biol Psychiatry*. (in press)
3. Ota M, Fujii T, Nemoto K, Tatsumi M, Moriguchi Y, Hashimoto R, Sato N, Iwata N, Kunugi H. A polymorphism of the ABCA1 gene confers susceptibility to schizophrenia and related brain changes. *Prog Neuropsychopharmacol Biol Psychiatry*. 35(8):1877-1883, 2011.12
4. Hashimoto R, Ohi K, Yasuda Y, Fukumoto M, Yamamori H, Kamino K, Morihara T, Iwase M, Kazui H, Takeda M. The KCNH2 gene is associated with neurocognition and the risk of schizophrenia. *World J Biol Psychiatry*. 2011.9 (epub)
5. Kazui H, Yoshida T, Takaya M, Sugiyama H, Yamamoto D, Kito Y, Wada T, Nomura K, Yasuda Y, Yamamori H, Ohi K, Fukumoto M, Iike N, Iwase M, Morihara T, Tagami S, Shimosegawa E, Hatazawa J, Ikeda Y, Uchida E, Tanaka T, Kudo T, Hashimoto R, Takeda M. Different Characteristics of Cognitive Impairment in Elderly Schizophrenia and Alzheimer's Disease in the Mild Cognitive Impairment Stage. *Dement Geriatr Cogn Disord* (in press)
6. Kushima I, Nakamura Y, Aleksic B, Ikeda M, Ito Y, Shiino T, Okochi T, Fukuo Y, Ujike H, Suzuki M, Inada T, Hashimoto R, Takeda M, Kaibuchi K, Iwata N, Ozaki N. Resequencing and Association Analysis of the KALRN and EPHB1 Genes And Their Contribution to Schizophrenia Susceptibility. *Schizophr Bull*, 2010.11(epub)
7. Ikezawa K, Ishii R, Iwase M, Kurimoto R, Canuet L, Takahashi H, Nakahachi T, Azechi M, Ohi K, Fukumoto M, Yasuda Y, Iike N, Takaya M, Yamamori H, Kazui H, Hashimoto R,

- Yoshimine T, Takeda M. Decreased alpha event-related synchronization in the left posterior temporal cortex in schizophrenia: A magnetoencephalography-beamformer study. *Neurosci Res*. 71(3):235-43, 2011.11
8. OHashimoto R, Ohi K, Yasuda Y, Fukumoto M, Yamamori H, Takahashi H, Iwase M, Okochi T, Kazui H, Saitoh O, Tatsumi M, Iwata N, Ozaki N, Kamijima K, Kunugi H and Takeda M. Variants of the *RELA* gene are associated with schizophrenia and their startle responses. *Neuropsychopharmacology*, 36(9):1921-1931, 2011.8
 9. Yamamori H, OHashimoto R, Verrall L, Yasuda Y, Ohi K, Fukumoto M, Umeda-Yano S, Ito A, Takeda M. Dysbindin-1 and NRG-1 gene expression in immortalized lymphocytes from patients with schizophrenia, *J Hum Genet*, 56(7):478-83, 2011.7
 10. Yasuda Y, OHashimoto R, Yamamori H, Ohi K, Fukumoto M, Umeda-Yano S, Mohri I, Ito A, Taniike M, Takeda M. Gene expression analysis in lymphoblasts derived from patients with autism spectrum disorder. *Molecular Autism*, 2:9, 2011.5
 11. OHashimoto R, Ohi K, Yasuda Y, Fukumoto M, Yamamori H, Kamino K, Morihara T, Iwase M, Kazui H, Numata S, Ikeda M, Ueno S, Ohmori T, Iwata N, Ozaki N, Takeda M. No association between the *PCMI* gene and schizophrenia: a multi-center case-control study and a meta-analysis. *Schizophrenia Res*, 129:80-84, 2011.6
 12. Yasuda Y, OHashimoto R, Ohi K, Fukumoto M, Umeda-Yano S, Yamamori H, Okochi T, Iwase M, Kazui H, Iwata N, Takeda M, Impact on schizotypal personality trait of a genome-wide supported psychosis variant of the *ZNF804A* gene, *Neurosci let*, 495:216-220, 2011.5
 13. Hashimoto H, Shintani N, Tanida M, Hayata A, O Hashimoto R, Baba A. PACAP is Implicated in the Stress Axes, *Curr Pharm Des, review*, 17(10):985-9, 2011.4
 14. Ohi K, Hashimoto R, Yasuda Y, Fukumoto M, Yamamori H, Umeda-Yano S, Kamino K, Ikezawa K, Azechi M, Iwase M, Kazui H, Kasai K, Takeda M. The *SIGMAR1* gene is associated with a risk of schizophrenia and activation of the prefrontal cortex. *Prog Neuropsychopharmacol Biol Psychiatry*, 35:1309-1315, 2011.4
 15. Kobayashi K, Umeda-Yano S, Yamamori H, Takeda M, Suzuki H, O Hashimoto R. Correlated Alterations in Serotonergic and Dopaminergic Modulations at the Hippocampal Mossy Fiber Synapse in Mice Lacking Dysbindin. *PLoS One*, 23;6(3):e18113, 2011.3
 16. Ikeda M, Aleksic B, Kinoshita Y, Okochi T, Kawashima K, Kushima I, Ito Y, Nakamura Y, Kishi T, Okumura T, Fukuo Y, Williams HJ, Hamshere ML, Ivanov D, Inada T, Suzuki M, O Hashimoto R, Ujike H, Takeda M, Craddock N, Kaibuchi K, Owen MJ, Ozaki N, O'Donovan MC, Iwata N. Genome-Wide Association Study of Schizophrenia in a Japanese Population. *Biol Psychiatry*, 69(5):472-478, 2011.3.
 17. Nihonmatsu-Kikuchi N, OHashimoto R, Hattori S, Matsuzaki S, Shinozaki T, Miura H, Ohta

S, Tohyama M, Takeda M, Tatebayashi Y. Reduced rate of neural differentiation in the dentate gyrus of adult dysbindin null (sandy) mouse. PLoS One, 18;6(1):e15886, 2011.1

研究分担者：大森崇

1. 高橋佳苗, 長尾能雅, 足立由起, 森本剛, 市橋則明, 坪山直生, ○大森崇, 佐藤俊哉 : 高齢者におけるベンゾジアゼピン系薬の服用量変更と転倒との関連 : 急性期病院入院患者を対象にした解析, 薬剤疫学 **16**, 11-20, 2011.
2. H.Sakaguchi, N.Ota, ○T.Omori, H.Kuwahara, T.Sozu, Y.Takagi, Y.Takahashi, K.Tanigawa, M.Nakanishi, T.Nakamura, T.Morimoto, S.Wakuri, Y.Okamoto, M.Sakaguchi, T.Hayashi, T.Hanji, S.Watanabe: Validation study of the Short Time Exposure (STE) test to assess the eye irritation potential of chemicals, Toxicology in Vitro **25**, 796-809, 2011.

V. 研究成果の刊行に関する別刷り
(平成 23 年度分)

Identification of Muscle-Specific MicroRNAs in Serum of Muscular Dystrophy Animal Models: Promising Novel Blood-Based Markers for Muscular Dystrophy

Hideya Mizuno¹, Akinori Nakamura², Yoshitsugu Aoki^{2,4}, Naoki Ito^{2,5}, Soichiro Kishi¹, Kazuhiro Yamamoto³, Masayuki Sekiguchi³, Shin'ichi Takeda², Kazuo Hashido^{1*}

1 Administrative Section of Radiation Protection, National Institute of Neuroscience, National Center of Neurology and Psychiatry, Kodaira, Tokyo, Japan, **2** Department of Molecular Therapy, National Institute of Neuroscience, National Center of Neurology and Psychiatry, Kodaira, Tokyo, Japan, **3** Department of Degenerative Neurological Diseases, National Institute of Neuroscience, National Center of Neurology and Psychiatry, Kodaira, Tokyo, Japan, **4** Department of System Neuroscience, Medical Research Institute, Tokyo Medical and Dental School University Graduate School, Tokyo, Japan, **5** Department of Biological Information, Tokyo Institute of Technology, Yokohama, Japan

Abstract

Duchenne muscular dystrophy (DMD) is a lethal X-linked disorder caused by mutations in the *dystrophin* gene, which encodes a cytoskeletal protein, dystrophin. Creatine kinase (CK) is generally used as a blood-based biomarker for muscular disease including DMD, but it is not always reliable since it is easily affected by stress to the body, such as exercise. Therefore, more reliable biomarkers of muscular dystrophy have long been desired. MicroRNAs (miRNAs) are small, ~22 nucleotide, noncoding RNAs which play important roles in the regulation of gene expression at the post-transcriptional level. Recently, it has been reported that miRNAs exist in blood. In this study, we hypothesized that the expression levels of specific serum circulating miRNAs may be useful to monitor the pathological progression of muscular diseases, and therefore explored the possibility of these miRNAs as new biomarkers for muscular diseases. To confirm this hypothesis, we quantified the expression levels of miRNAs in serum of the dystrophin-deficient muscular dystrophy mouse model, *mdx*, and the canine X-linked muscular dystrophy in Japan dog model (CXMD_J), by real-time PCR. We found that the serum levels of several muscle-specific miRNAs (miR-1, miR-133a and miR-206) are increased in both *mdx* and CXMD_J. Interestingly, unlike CK levels, expression levels of these miRNAs in *mdx* serum are little influenced by exercise using treadmill. These results suggest that serum miRNAs are useful and reliable biomarkers for muscular dystrophy.

Citation: Mizuno H, Nakamura A, Aoki Y, Ito N, Kishi S, et al. (2011) Identification of Muscle-Specific MicroRNAs in Serum of Muscular Dystrophy Animal Models: Promising Novel Blood-Based Markers for Muscular Dystrophy. PLoS ONE 6(3): e18388. doi:10.1371/journal.pone.0018388

Editor: Sebastien Pfeffer, French National Center for Scientific Research - Institut de biologie moléculaire et cellulaire, France

Received: October 27, 2010; **Accepted:** March 6, 2011; **Published:** March 30, 2011

Copyright: © 2011 Mizuno et al. This is an open-access article distributed under the terms of the Creative Commons Attribution License, which permits unrestricted use, distribution, and reproduction in any medium, provided the original author and source are credited.

Funding: This work was supported by the Health and Labour Sciences Research Grants for Translational research from the ministry of Health, Labour and Welfare of Japan. The funders had no role in study design, data collection and analysis, decision to publish, or preparation of the manuscript.

Competing Interests: The authors have declared that no competing interests exist.

* E-mail: hashido@ncnp.go.jp

Introduction

Duchenne muscular dystrophy (DMD) is a lethal X-linked disorder caused by mutations in the *dystrophin* gene, which encodes a cytoskeletal protein, dystrophin[1]. The absence of dystrophin results in progressive degeneration of skeletal and cardiac muscle with fibrotic tissue replacement, fatty infiltration, and subsequent early death by respiratory or heart failure[2,3]. Creatine kinase (CK) is an enzyme related to energy metabolism present in various types of cells[4]. CK is commonly used as a blood-based biomarker for muscular dystrophy to evaluate the level of muscle damage and necrosis, and the efficacy of potential therapies, but it is not always reliable since it is easily affected by stress to the body, such as exercise[5,6,7]. Other markers for muscular dystrophy, such as myoglobin, aldolase or lactate dehydrogenase, also have the same problem. Therefore, more reliable biomarkers of muscular dystrophy have long been desired.

MicroRNAs (miRNAs) are small, ~22 nucleotide, noncoding RNAs which play important roles in the regulation of gene expression at the post-transcriptional level[8]. Recently, it has been reported that specific miRNAs in blood are promising biomarkers

for cancer, liver injury and heart failure [9,10,11]. These studies showed that the levels of specific circulating miRNAs are associated with the development of these pathological processes. It has also been reported that miRNAs are released from cells through an exosomal-mediated pathway[12], suggesting that circulating miRNAs are packaged in exosomes, which protects them from RNases.

We hypothesized that the expression levels of specific serum circulating miRNAs may be useful to monitor the pathological progression of muscular diseases, and therefore explored the possibility of these miRNAs as new biomarkers for muscular diseases. Here, we demonstrate that the serum levels of several muscle-specific miRNAs are increased in the dystrophin-deficient muscular dystrophy mouse model, *mdx*, as well as the canine X-linked muscular dystrophy in Japan dog model (CXMD_J) [13,14,15]. These results suggest that serum miRNAs are useful as markers for muscular dystrophy.

Results

To explore the possibility of miRNA as a biomarker for DMD, we quantified the expression levels of several miRNAs in the serum

of *mdx* by real-time PCR. The expression levels of miRNAs are indicated as either cycle threshold (Ct) (**Figure 1a**) or fold expression compared to wild-type (**Figure S1**). The Ct values of the ubiquitously expressed miR-16, brain-rich miR-132 [16] and small nucleolar RNA 202 (sno202) did not show any significant differences between wild-type and *mdx* serum (**Figure 1a**). In contrast, muscle-specific miR-1, -133a and -206 [17,18,19] were significantly increased in *mdx* (**Figure 1a**). The expression levels of these miRNAs in *mdx* were 10- to 100-fold higher than in wild-type controls (**Figure S1**). In Figure 1, the data are shown without normalization by an internal control RNA. Although small nuclear RNA U6, sno202 and ubiquitously expressed miRNA, such as miR-16, are often used as an internal control for miRNA analysis, there is currently no consensus for a serum internal control miRNA for real-time PCR analysis. Indeed, we examined the expression of U6 but found it was undetectable in serum (data not shown), and sno202 and miR-16 revealed no significant difference between wild-type and *mdx* (**Figure 1a** and **Figure S1**). In addition, miR-16 was more abundant than sno202 in serum (**Figure 1a**). Therefore, we employed miR-16 as the internal control for normalization of muscle-specific miRNAs in serum in the subsequent studies.

We also confirmed the accuracy of miR-16 as an internal control by using exogenous miRNA (spiked-in miRNA). *C. elegans* miRNA-39 (cel-miR-39) was used as a spiked-in miRNA because of the lack of sequence homology to mouse miRNAs. Synthetic cel-miR-39 was spiked into serum after the addition of denaturing solution including RNase inhibitors. Then, miRNAs were isolated and the levels of cel-miR-39, miR-16, -1, -133a and -206 were determined by real-time PCR (**Figure S2**). In three-repeated experiments, the quantities of cel-miR-39 and miR-16 showed similar levels each time (**Figure S2a**). Furthermore, the expression levels of miR-1, -133a and -206 were calculated by normalization with cel-miR-39 or miR-16, individually (**Figure S2b**). The expression levels of miR-1, -133a and -206 were highly elevated in *mdx*, and the results were consistent between normalization with cel-miR-39 and miR-16.

It is conceivable that leakage or secretion from skeletal muscle fibers is the major cause of the increase in muscle-specific miRNAs in serum, but there remains the possibility that these miRNAs are excessively expressed in dystrophic skeletal muscle, which then influences serum expression levels. To investigate this possibility, we examined the expression level of these miRNAs in the skeletal muscle (soleus: Sol, tibialis anterior: TA and diaphragm: DIA) of *mdx* (**Figure S3**). Levels of ubiquitously expressed miR-16 were not different among the muscles examined, but miR-1 and miR-133a were significantly decreased in Sol and TA of *mdx*, although the differences are less than 2-fold. On the other hand, miR-206 was significantly increased in *mdx* TA and DIA, but not in Sol, and this increase of miR-206 in some *mdx* muscles could be related to a previously reported role for miR-206 in muscle regeneration[20]. Since miR-1 and -133a levels were highly elevated in *mdx* serum, although they were not increased in *mdx* skeletal muscle, suggests that the increase of muscle-specific miRNAs in *mdx* serum is caused by an increase in leakage or secretion of miRNAs from muscle.

Since it is very important to investigate whether muscle-specific miRNA levels are affected by exercise like as CK, we compared CK and miRNA levels in mice serum after exercise using a treadmill. Both CK and miRNA were increased after the treadmill exercise (**Figure 1b**, left, normalized to wild-type control), however miRNAs appeared to be less affected. When the increase in miRNAs were corrected by the data before exercise in each group (**Figure 1b**, right, normalized by each control), CK showed

almost a 60-fold increase after exercise, whereas the change of muscle-specific miRNA levels was less than 10-fold.

CXMD_J is a well characterized dog model of DMD, which shows severe and progressive symptoms[13,14,15]. We therefore analyzed the expression levels of miRNAs in normal, carrier (females possessing a mutant *dystrophin* gene on one of two X-chromosomes) and CXMD_J dog serum at various ages. The Ct value of these miRNAs in CXMD_J was significantly smaller than age-matched controls (**Figure S4**). Relative expression levels corrected by miR-16 are shown in **Figure 2**. These miRNAs are apparently able to distinguish CXMD_J from age-matched normal dogs. Shimatsu *et al.* previously reported that the CK concentration of CXMD_J dogs do not increase with age [21]. Thus, our results of these miRNA levels are consistent with the CK levels in this model.

Our data indicate that the levels of miR-1, -133a and -206 relative to miR-16 are increased in the serum of two animal models of muscular dystrophy, *mdx* and CXMD_J. It is very intriguing that serum miRNA were less affected by stress, such as exercise, compared with CK. In conclusion, muscle-specific miRNAs in serum may be useful biological markers for muscular dystrophy which are more reliable than CK, and further investigations are required to clarify the molecular mechanisms by which miRNAs are released from the inside of cells into serum.

Discussion

Recently, several studies have reported that miRNAs in serum are promising biomarkers for diseases, such as cancers, liver injury or heart failure [9,10,11]. CK is commonly used as a biomarker of muscular diseases to evaluate the level of muscle damage and necrosis, and the efficacy of potential therapies, but it is not always reliable since it is easily affected by stress to the body, such as exercise [5,6,7]. Therefore, more reliable biomarkers of muscular dystrophy have long been desired. We hence investigated whether serum miRNAs are useful for monitoring the pathological condition of muscular diseases. In this report, we demonstrate that the serum levels of several muscle-specific miRNAs are increased in two dystrophin-deficient muscular dystrophy animal models. Importantly, we show that the levels of these miRNAs are much less affected by stress to the body compared with CK levels.

To investigate the mechanism of the increase of miRNA expression, we also examined the expression level of miR-1, miR-133a and miR-206 in the skeletal muscle of *mdx* (**Figure S3**). miR-1 and -133a were significantly decreased in Sol and TA of *mdx*. On the other hand, miR-206 was significantly increased in TA and DIA of *mdx*. Our results suggest that the increase of muscle-specific miRNAs in the serum of these DMD models is caused by an increase in leakage or secretion of miRNAs from muscle, and not by the change of expression in skeletal muscle. However, it is not yet clear whether the increase of these miRNAs is caused by leakage or secretion from muscle. It is conceivable that leakage from skeletal muscle fibers is the major cause of the increase in muscle-specific miRNAs in *mdx* serum, but it is hard to explain why these miRNAs were not degraded by RNase. Mitchell *et al.* [10] showed that synthetic miRNAs are immediately degraded in serum even though endogenous circulating miRNAs are stably expressed in serum. To explain these results, they suggested that miRNAs are released from cells through an exosomal-mediated pathway. If circulating miRNAs are secreted by an exosomal-mediated pathway, it is possible that dystrophin is involved in the regulation of exosome secretion and a lack of dystrophin results in increased miRNA release. However, further investigation is required to clarify the contribution of dystrophin in exosome secretion.

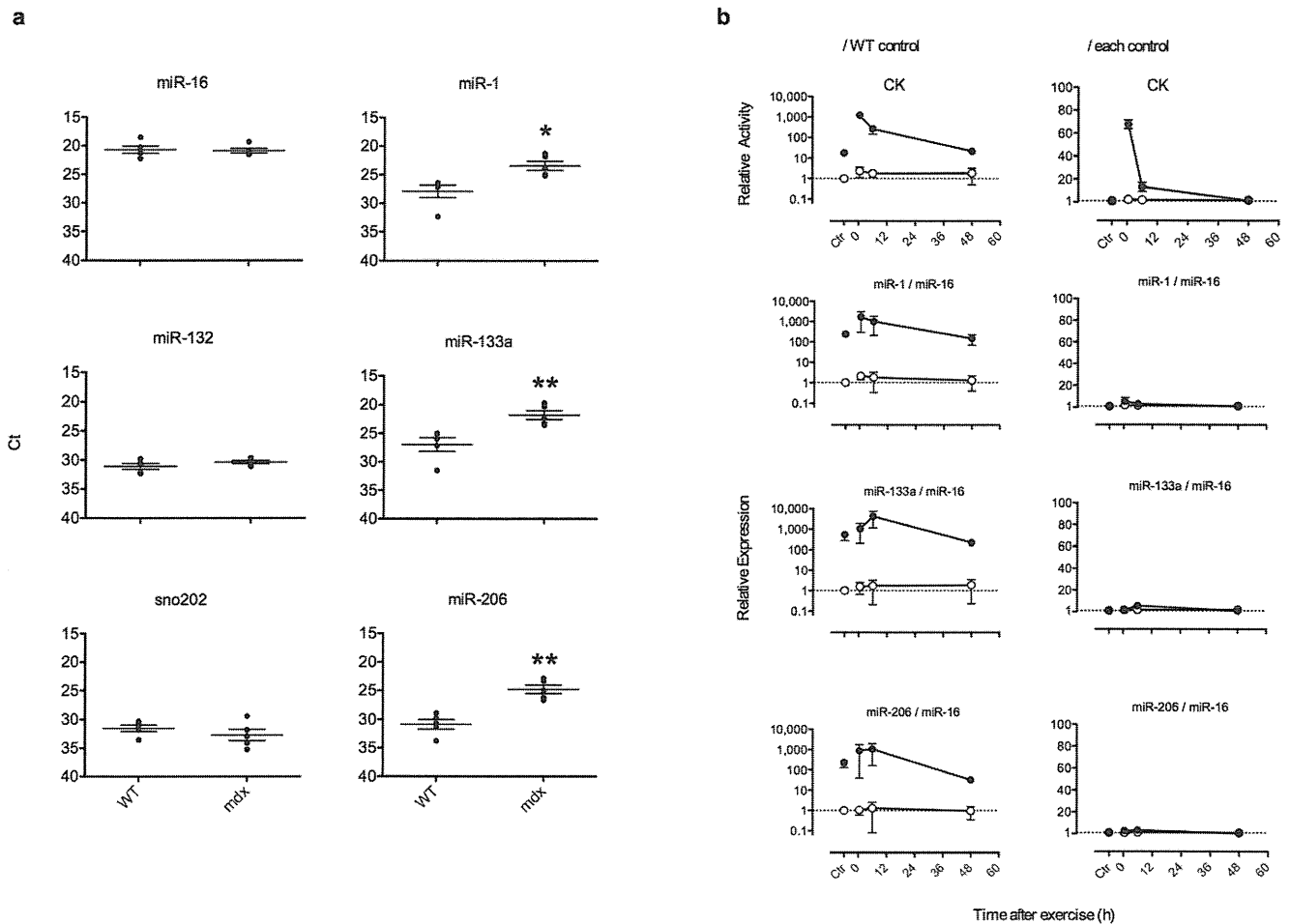


Figure 1. Elevation of muscle-specific miRNA levels in *mdx* mouse serum. (a) Expression levels of miRNAs in 8-week old male wild-type and *mdx* serum. Ct was determined by real-time PCR. In these graphs, the longer bars on each plot indicate the mean, and the shorter bars indicate \pm SEM, $n=5$. Asterisk (*) indicates a significant difference (*, $P<0.05$; **, $P<0.01$, two-tailed Student's t-test). The actual P value for each test was $P=0.797$ (miR-16), 0.222 (miR-132), 0.344 (sno202), 0.011 (miR-1), 0.007 (miR-133a) and 0.001 (miR-206). (b) CK and miRNA expression levels in wild-type and *mdx* serum after treadmill exercise. Running on the treadmill was continued for 20 min. About 100 μ l of blood was collected from the tail vein at 0.5, 6 and 48 h after the exercise. Six days before the test, blood was collected as a control. Expression levels were normalized to the wild-type control (left) or each individual control (right). Data are presented as mean \pm SEM, $n=3$. \circ : wild-type; \bullet : *mdx*. doi:10.1371/journal.pone.0018388.g001

The change of miRNA expression levels in skeletal muscle of *mdx* in this report is consistent with previous reports [20,22]. It is intriguing that TA muscle of denervated mice also showed an increase in miR-206 and a decrease in miR-1 and -133a [23]. Yuasa *et al.* [20] also showed that miR-206 expression was increased after cardiotoxin-induced muscle regeneration and that miR-206 contributes to muscle regeneration. Interestingly, it has been showed that the expression levels of miR-206 in DMD patients are not increased [24] or that the increase is not as large as in *mdx* [22]. Although *mdx* mice are deficient in dystrophin, they do not show lethality unlike in humans. Increased miR-206 expression levels in *mdx* therefore contribute to the different phenotype between humans and mice. In addition, Williams *et al.* [23] showed that expression of miR-206 delays disease progression and promotes regeneration of neuromuscular synapses in amyotrophic lateral sclerosis (ALS) model mice. Taken together, these results indicate that gene therapy using miR-206 may be a useful treatment for muscular diseases.

In this report, we focused on muscle-specific miRNAs and found that they are significantly increased in serum of DMD models. To investigate whether such an increase can be observed

in some myopathy models which do not have any effective diagnosis markers, we also measured these muscle-specific miRNAs in serum of steroid treated dogs. We found that serum level of miR-1, -133a and -206 were not increased in steroid treated dog did not show increase compared with non-treatment controls (data not shown). Intriguingly, Lodes *et al.* [25] performed microarray analysis with circulating miRNAs and found an increase in specific miRNAs in serum of cancer patients. Furthermore the miRNA expression patterns were able to discriminate between healthy controls and cancer patients. Such a microarray analysis may be useful for identifying diagnosis markers for muscular diseases for which effective diagnosis markers currently do not exist.

Materials and Methods

Ethics Statement

The dog study was approved by the Ethics Committee for the Treatment of Middle-sized Laboratory Animals of the National Institute of Neuroscience, National Center of Neurology and Psychiatry, approval ID: 21-02 and 22-02. The mice study was

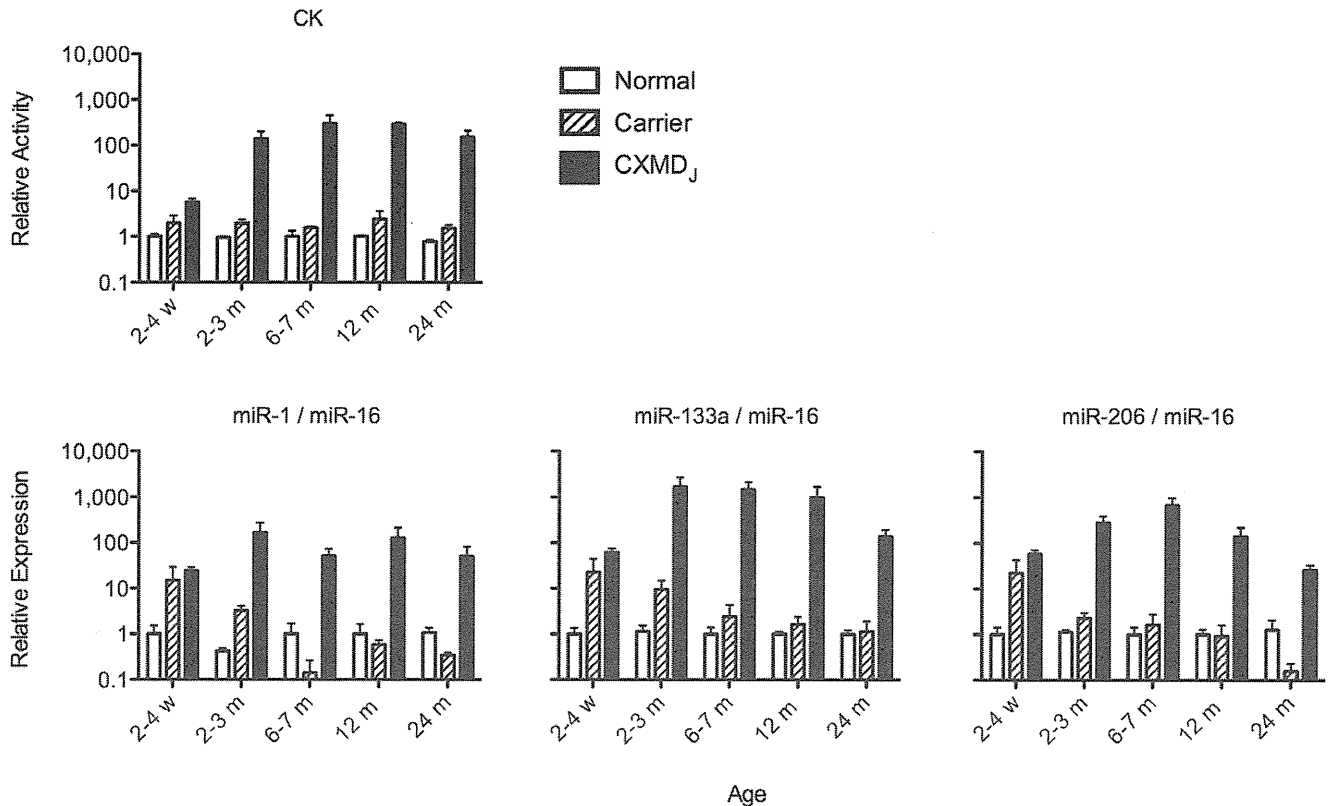


Figure 2. Elevation of muscle-specific miRNAs in CXMD_J dog serum. CK activity and miRNA expression in the serum of normal, carrier and dystrophy dogs (CXMD_J) at the indicated ages were determined. Expression levels of miR-1, miR-133a, miR-206 and miR-16 were determined by real-time PCR, and levels of each muscle-specific miRNA (miR-1, miR-133a and miR-206) was corrected by miR-16 levels. Results are indicated as relative expression to normal dogs at each age, and are presented as mean \pm SEM, $n=3$. w: weeks; m: months. doi:10.1371/journal.pone.0018388.g002

approved by the Ethics Committee for the Treatment of Laboratory Animals of the National Institute of Neuroscience, National Center of Neurology and Psychiatry, approval ID: 2008011.

Animals and serum samples

All animals in this study were cared for and treated in accordance with the guidelines provided by the Ethics Committee for the Treatment Laboratory Animals of National Institute of Neuroscience, or the Ethics Committee for the Treatment Laboratory Middle-sized Animals of National Institute of Neuroscience. Skilled experimental animal technicians, who have special knowledge of methods to prevent unnecessary excessive pain, handled the animals and assisted in the experiments.

As Duchenne muscular dystrophy (DMD) models, the X-chromosome-linked muscular dystrophy (*mdx*) mouse and canine X-linked muscular dystrophy in Japan (CXMD_J), Beagle-based medium-sized dystrophic dogs, were used in this study. In **Figure 1a**, whole body blood of male *mdx* mice ($n=5$) or age-matched controls (strain C57BL/10; B10) ($n=5$) at 8 weeks were collected from the abdominal vena cava under anesthesia. Blood collection after the treadmill test (**Figure 1b**), was performed from the tail vein of *mdx* ($n=3$) or age-matched control ($n=3$) under anesthesia. The phenotype of CXMD_J has been reported previously [13,14,15]. For analysis of the serum of CXMD_J dogs, mutation carrier female dogs and wild-type control dogs ($n=3$, at each age indicated in Figure 2), blood was collected from the subcutaneous vein of the hindlimb, and whole blood was allowed

to stand for about 1 h at room temperature before centrifugation at 1,800 g for 10 min at room temperature. The resultant serum was dispensed into a 1.5 ml cryotube and stored at -80°C until use.

RNA isolation and quantification of miRNA

Total RNA, including miRNA, was extracted from 50 μl of serum using the mirVana miRNA isolation kit (Ambion, Austin, TX, USA) according to the manufacturer's instructions, and finally eluted with 50 μl of elution buffer provided by the manufacturer. Five μl of total RNA was reverse transcribed using the TaqMan miRNA Reverse Transcription kit (Applied Biosystems, Foster City, CA, USA) and miRNA-specific stem-loop primers (part of TaqMan miRNA assay kit; Applied Biosystems). The expression levels of miRNA were quantified by real-time PCR using individual miRNA-specific primers (part of TaqMan miRNA assay kit; Applied Biosystems) with 7900HT Fast Real-Time PCR System (Applied Biosystems) according to the manufacturer's instructions. There is no current consensus on the use of an internal control for real-time PCR analysis of serum miRNA. Therefore, we used fixed volumes of starting serum (50 μl), buffer for the elution of RNA (50 μl) from starting serum, and input into the RT reaction (5 μl) in each assay for technical consistency. Data analysis was performed by SDS 2.1 real-time PCR data analysis software (Applied Biosystems). Threshold was fixed at 0.2 in each analysis for data consistency. The similarities of linearity of primers for each target miRNA were confirmed by using a dilution series of synthetic miRNAs.

Spiked-in miRNA experiment

We followed the protocol previously reported by Mitchell *et al.* [10] to determine endogenous miRNA levels with spiked-in miRNA. Spiked-in miRNA was designed against *C. elegans* microRNA-39 (cel-miR-39)(5'-UCACCGGGUGUAAAUCAGCUU-3'), and was synthesized by Sigma Aldrich Japan. Synthetic cel-miR-39 was spiked into serum after the addition of denaturing solution including RNase inhibitors. Isolation of total RNA, including miRNA, and quantification of the expression levels of miRNAs by real-time PCR were performed as described above.

Creatine kinase determination

Serum creatine kinase (CK) levels were assayed with the Fuji Drychem system (Fuji Film Medical Co. Ltd, Tokyo, Japan) according to the manufacturer's instructions. Data was expressed as units per liter (U/l).

Treadmill test

Mice were forced to run on a treadmill (MK-680S treadmill: Muromachi Kikai, Tokyo, Japan) with an inclination of 0° at 5 m/min for 5 min. Then, the speed was increased by 1 m/min every minute for a further 15 min. After the running, blood was immediately collected from the tail vein, as well as subsequently collected at the indicated times.

Statistics

Statistical significances between groups were determined by the two-tailed t-test, or one-way ANOVA with Bonferroni post hoc test. Each analysis was performed by Prism 5 (Graphpad Software Inc., San Diego, CA, USA).

Supporting Information

Figure S1 miRNA expression in 8-week old male wild-type control and *mdx* serum. Expression levels of miRNAs were determined by real-time PCR. Results are shown as relative expression, and data are presented as mean \pm SEM, $n = 5$. (TIFF)

Figure S2 (a) Confirmation of the consistency of miRNA isolation from serum. *C. elegans* miR-39 (cel-miR-39) was chemically synthesized and added to the denatured mouse serum samples. Total RNA was isolated from the mouse serum samples,

References

- Moser H (1984) Duchenne muscular dystrophy: pathogenetic aspects and genetic prevention. *Hum Genet* 66: 17–40.
- Cullen MJ, Mastaglia FL (1980) Morphological changes in dystrophic muscle. *Br Med Bull* 36: 145–152.
- Ervasti JM, Ohlendieck K, Kahl SD, Gaver MG, Campbell KP (1990) Deficiency of a glycoprotein component of the dystrophin complex in dystrophic muscle. *Nature* 345: 315–319.
- Ebashi S, Toyokura Y, Momoi H, Sugita H (1959) High creatine phosphokinase activity of sera of progressive muscular dystrophy. *J Biochem* 46: 103–104.
- Vassella F, Richterich R, Rossi E (1965) The Diagnostic Value of Serum Creatine Kinase in Neuromuscular and Muscular Disease. *Pediatrics* 35: 322–330.
- Florence JM, Fox PT, Planer GJ, Brooke MH (1985) Activity, creatine kinase, and myoglobin in Duchenne muscular dystrophy: a clue to etiology? *Neurology* 35: 758–761.
- Nicholson GA, Morgan GJ, Meerkin M, Strauss ER, McLeod JG (1986) The effect of aerobic exercise on serum creatine kinase activities. *Muscle Nerve* 9: 820–824.
- Chen K, Rajewsky N (2007) The evolution of gene regulation by transcription factors and microRNAs. *Nat Rev Genet* 8: 93–103.
- Ji X, Takahashi R, Hiura Y, Hirokawa G, Fukushima Y, et al. (2009) Plasma miR-208 as a Biomarker of Myocardial Injury. *Clin Chem* 55: 1944–1949.
- Mitchell PS, Parkin RK, Kroh EM, Fritz BR, Wyman SK, et al. (2008) Circulating microRNAs as stable blood-based markers for cancer detection. *Proc Natl Acad Sci USA* 105: 10513–10518.

and the quantity of exogenous cel-miR-39 and endogenous miR-16 were determined by real-time PCR. (b) Expression levels of miR-1, -133a and -206 in wild-type control and *mdx* serum, which were individually normalized by the cel-miR-39 spiked-in control or the endogenous control, miR-16. Results are shown as relative expression. The longer bars on each plot indicate the mean, and the shorter bars indicate \pm SEM, $n = 3$.

(TIFF)

Figure S3 miRNA expression in wild-type control and *mdx* muscles. Expression levels of miR-1, -16, -133a and -206 in Soleus (Sol), tibialis anterior (TA) and diaphragm (DIA) were determined by real-time PCR. Results are shown as relative expression. sno202 was used as an internal control. Data are presented as mean \pm SEM, $n = 4$. Asterisk (*) indicates a significant difference (*, $P < 0.05$; $P < 0.01$, two-tailed Student's t-test). The actual P value for each test was $P = 0.024$ (miR-1) and 0.010 (miR-206) in Sol; $P = 0.002$ (miR-1), 0.008 (miR-133a) and < 0.001 (miR-206) in TA; $P = 0.006$ (miR-206) in DIA.

(TIFF)

Figure S4 Expression levels of muscle-specific miRNAs in the serum of normal, carrier and dystrophy dogs (CXMD_J) at the indicated ages. Each Ct was determined by real-time PCR. In these graphs, the longer bars on each plot indicate the mean, and the shorter bars indicate \pm SEM, $n = 3$. Asterisk (*) and pound (#) indicate a significant difference (*, $P < 0.05$; **, $P < 0.01$; ***, $P < 0.001$ from normal: #, $P < 0.05$; ##, $P < 0.01$; ###, $P < 0.001$ from carrier, one-way ANOVA with Bonferroni post hoc test). w: weeks; m: months.

(TIFF)

Acknowledgments

We would like to thank T. Yokota, M. Mori and K. Yuasa for critical feedback on the manuscript; M. Kobayashi, H. Kita, S. Ichikawa, Y. Yahata, T. Nakayama, K. Kinoshita, R. Nakagawa and Y. Kasahara (Department of Molecular Therapy) for assistance with the experiments.

Author Contributions

Conceived and designed the experiments: HM AN ST KH. Performed the experiments: HM YA NI SK. Analyzed the data: HM KH. Contributed reagents/materials/analysis tools: KY MS AN. Wrote the paper: HM.

19. McDanel TG, Smith TPL, Doumit ME, Miles JR, Coutinho LL, et al. (2009) MicroRNA transcriptome profiles during swine skeletal muscle development. *BMC Genomics* 10: 77.
20. Yuasa K, Hagiwara Y, Ando M, Nakamura A, Takeda Si, et al. (2008) MicroRNA-206 is highly expressed in newly formed muscle fibers: implications regarding potential for muscle regeneration and maturation in muscular dystrophy. *Cell Struct Funct* 33: 163–169.
21. Shimatsu Y, Yoshimura M, Yuasa K, Urasawa N, Tomohiro M, et al. (2005) Major clinical and histopathological characteristics of canine X-linked muscular dystrophy in Japan. *CXMDJ. Acta Myol* 24: 145–154.
22. Greco S, De Simone M, Colussi C, Zaccagnini G, Fasanaro P, et al. (2009) Common micro-RNA signature in skeletal muscle damage and regeneration induced by Duchenne muscular dystrophy and acute ischemia. *Faseb J* 23: 3335–3346.
23. Williams AH, Valdez G, Moresi V, Qj X, McAnally J, et al. (2009) MicroRNA-206 delays ALS progression and promotes regeneration of neuromuscular synapses in mice. *Science* 326: 1549–1554.
24. Eisenberg I, Eran A, Nishino I, Moggio M, Lamperti C, et al. (2007) Distinctive patterns of microRNA expression in primary muscular disorders. *Proc Natl Acad Sci U S A* 104: 17016–17021.
25. Lodes MJ, Caraballo M, Suci D, Munro S, Kumar A, et al. (2009) Detection of cancer with serum miRNAs on an oligonucleotide microarray. *PLoS ONE* 4: e6229.



Reactive gliosis of astrocytes and Müller glial cells in retina of POMGnT1-deficient mice

Hisatomo Takahashi^a, Hironori Kanesaki^{b,c}, Tsutomu Igarashi^d, Shuhei Kameya^{a,*}, Kunihiro Yamaki^a, Atsushi Mizota^e, Akira Kudo^b, Yuko Miyagoe-Suzuki^c, Shin'ichi Takeda^c, Hiroshi Takahashi^d

^a Department of Ophthalmology, Nippon Medical School Chiba Hokusoh Hospital, 1715 Kamagari, Inzai, Chiba 270-1694, Japan

^b Department of Biological Information, Tokyo Institute of Technology, 4259 Nagatsuta, Midori-ku, Yokohama 226-8501, Japan

^c Department of Molecular Therapy, National Institute of Neuroscience, National Center of Neurology and Psychiatry, 4-1-1 Ogawahigashi, Kodaira, Tokyo 187-8502, Japan

^d Department of Ophthalmology, Nippon Medical School, 1-1-5 Sendagi, Bunkyo-ku, Tokyo 113-8602, Japan

^e Department of Ophthalmology, Teikyo University of Medicine, 2-11-1 Kaga, Itabashi-ku, Tokyo 173-8605, Japan

ARTICLE INFO

Article history:

Received 19 November 2010

Revised 5 March 2011

Accepted 21 March 2011

Available online 8 April 2011

Keywords:

Muscle–eye–brain disease

Dystroglycan

Retinal detachment

ABSTRACT

Protein O-linked mannanose beta1, 2-N-acetylglucosaminyltransferase 1 (POMGnT1) is an enzyme that catalyzes the transfer of N-acetylglucosamine to O-mannose of glycoproteins. Alpha-dystroglycan, a substrate of POMGnT1, is concentrated around the blood vessels, in the outer plexiform layer (OPL), and in the inner limiting membrane (ILM) of the retina. Mutations of the *POMGnT1* gene in humans cause muscle-eye-brain (MEB) disease. Several ocular abnormalities including retinal dysplasia, ERG abnormalities, and retinal detachments have been reported in patients with MEB. We have analyzed the eyes of POMGnT1-deficient mice, generated by standard gene targeting technique, to study the retinal abnormalities. Clinical examination of adult mutant mice revealed a high incidence (81% by 12-months-of-age) of retinal detachments. Sheathing of the retinal vessels and the presence of ectopic fibrous tissues around the optic nerve head were also found. Histological examinations showed focal retinal detachment associated with GFAP immunopositivity. The ILM of the mutant mice was disrupted with ectopic cells near the disruptions. The expression of Dp71, a shorter isoform of dystrophin, was severely reduced in the ILM and around retinal blood vessels of POMGnT1-deficient mice. The expression of Dp427, Dp260, Dp140 were also reduced in the OPL of the mutant mice. Electroretinographic (ERG) analyses showed reduced a- and b-wave amplitudes. Examinations of flat mounts revealed abnormal vascular network associated with highly irregular astrocytic processes. In addition, ER-TR7-positive fibrous tissue was found closely associated with reactive astrocytes especially around the optic nerve head. Our results suggest that altered glycosylation of alpha-DG may be responsible for the reactive gliosis and reticular fibrosis in the retina, and the subsequent developments of retinal dysplasia, abnormal ERGs, and retinal detachment in the mutant mice.

© 2011 Elsevier Inc. All rights reserved.

Introduction

Protein O-linked mannanose beta1, 2-N-acetylglucosaminyltransferase 1 (POMGnT1) is an enzyme that catalyzes the transfer of N-acetylglucosamine to O-mannose of glycoproteins (Yoshida et al., 2001). Mutations of the *POMGnT1* gene cause muscle–eye–brain (MEB) disease, one of a family of dystroglycanopathies, in humans (Yoshida et al., 2001). The dystroglycanopathies include a group of muscular dystrophies including Walker-Warburg syndrome (WWS), Fukuyama-type congenital muscular dystrophy (FCMD), congenital muscular dystrophy (MDC) 1C/D, limb-girdle muscular dystrophy (LGMD) 2I/K/M/N, and MEB. This group of disorders is clinically characterized by various combinations of severe muscular dystrophy, mental retardation,

and ocular abnormalities. To date, mutations in six known or putative glycosyltransferase genes, viz., *POMT1*, *POMT2*, *Fukutin*, *FKRP*, *LARGE*, and *POMGnT1*, have been identified to be associated with these disorders (Beltrán-Valero de Bernabé et al., 2002; van Reeuwijk et al., 2005; Kobayashi et al., 1998; Brockington et al., 2001; Longman et al., 2003). A common molecular defect for the dystroglycanopathies is the post-translational modification or hypoglycosylation of alpha-dystroglycan (alpha-DG).

Dystroglycan (DG) is encoded by a single gene and is cleaved into two proteins, alpha-DG and beta-DG, by post-translational processing (Ibraghimov-Beskrovnaya et al., 1992). Alpha-DG is a heavily glycosylated glycoprotein and is a central component of the dystrophin glycoprotein complex (DGC). A major function of the DGC is to link cytoskeletal actin to the basal lamina which maintains the structural integrity of skeletal muscles (Ervasti and Campbell, 1993). Mutations in the components of DGC cause various forms of muscular dystrophies (Straub and Campbell, 1997).

* Corresponding author. Fax: +81 476 99 1923.

E-mail address: shuheik@nms.ac.jp (S. Kameya).

DG and other components of DGC are widely expressed in the CNS and the retina (Henry and Campbell, 1999; Blake and Kröger, 2000). Alpha-DG functions as a cell surface receptor for laminin, perlecan, agrin, neuroligin, and pikachurin in a variety of tissues (Ervasti and Campbell, 1993; Gee et al., 1994; Peng et al., 1998; Sugita et al., 2001; Sato et al., 2008).

In the retina, alpha-DG is concentrated in the inner limiting membrane (ILM), around blood vessels, and in the outer plexiform layer (OPL; Blake and Kröger, 2000). The alpha-DG in the ILM is concentrated at the endfeet of the Müller cells, and that in the blood vessels in the perivascular astrocytes (Montanaro et al., 1995; Claudepierre et al., 1999). The alpha-DG in the OPL is localized around the site of expression of ribbon synapses of rod and cone photoreceptor terminals (Ueda et al., 1995; Montanaro et al., 1995).

Abnormal electroretinograms (ERGs) have been recorded from patients with MEB disease (Pihko et al., 1995; Fahnehjelm et al., 2001), and have frequently been recorded from individuals with Duchenne and Becker muscular dystrophies (Pillers et al., 1999). The findings in several mouse models with disruption of dystrophin, *Large^{vis}* and fukutin indicated that DGC is associated with the normal physiology of the retina (Pillers et al., 1995; Kameya et al., 1997; Lee et al., 2005; Takeda et al., 2003). Abnormal ERGs in mice with a targeted disruption of pikachurin, an extracellular ligand of alpha-dystroglycan at ribbon synapses, also support the idea that DGC must be present in the OPL for normal retinal physiology (Sato et al., 2008).

It was recently shown that inactivation of glial specific dystroglycan, located in the endfeet of Müller cells and perivascular astrocytes, led to a reduction of the b-wave of the ERG. This suggested that glial specific

dystroglycan also plays an important role in the normal physiology of the retina (Satz et al., 2009).

Patients with MEB have a variety of ocular abnormalities including myopia, glaucoma, anterior chamber malformation, microphthalmia, buphthalmus, nystagmus, strabismus, cataract, chorioretinal atrophy, retinal dysplasia, and retinal detachment (Cormand et al., 2001; Mercuri et al., 2009). The purpose of this study was to determine the effect of altered glycosylation of alpha-DG caused by inactivation of POMGnT1 in the retina. To accomplish this, we studied mice with targeted disruption of the *POMGnT1* gene. We shall show that *POMGnT1*-deficient mice have a high incidence of retinal detachment with reactive gliosis of the Müller glial cells and the perivascular astrocytes. Our results suggest that altered glycosylation of alpha-DG may be responsible for the retinal dysplasia, abnormal ERGs, and retinal detachment in humans with MEB.

Results

Retinal detachment in *POMGnT1*-deficient mice

At 6-weeks-of-age, the retinal vessels of all *POMGnT1*-deficient mice were tortuous but none of the mice had a retinal detachment (Fig. 1B). These mutant mice also had fibrous tissue over the retina especially around the optic nerve head (Fig. 1B). Fibrous tissues were not observed in any of the wild type mice.

By 6-months-of-age, the retinal vessels were sheathed, and focal and extensive retinal detachments were present in the areas of the sheathed vessels (Fig. 1C). The retinal detachment of some of the mice covered

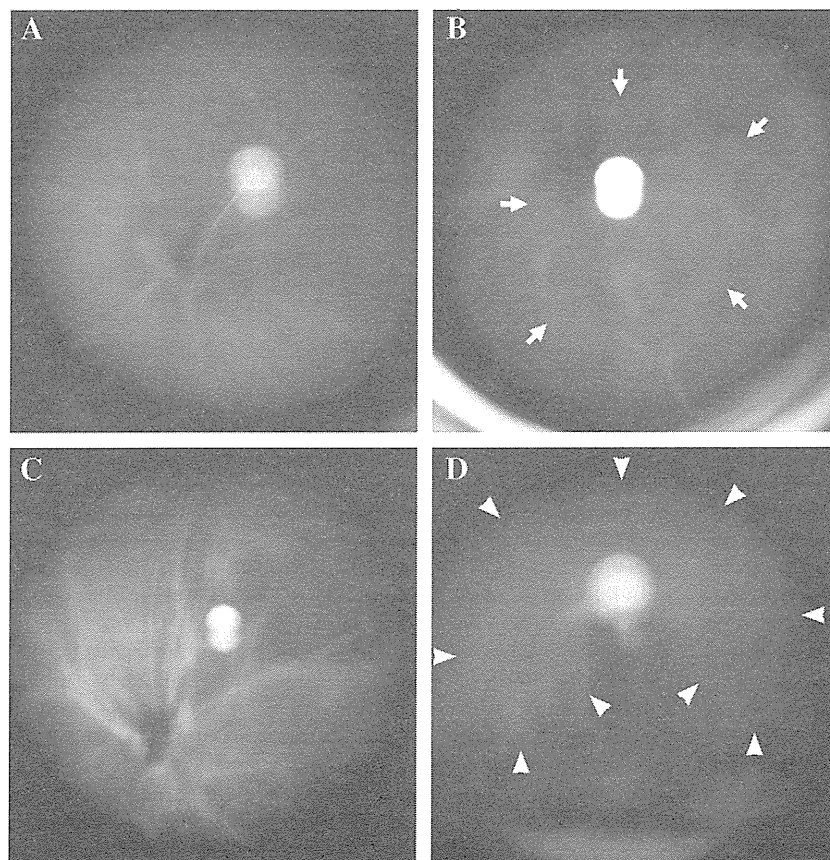


Fig. 1. Fundus photograph of wild-type and *POMGnT1*-deficient mice. A. Six-week-old wild type mouse. B. Retinal vessel tortuosity can be seen in this 6-week-old *POMGnT1*-deficient mouse. Arrows point to ectopic fibrous tissue surrounding the optic nerve head. C. Six-month-old *POMGnT1*-deficient mouse showing sheathing of the retinal vessels. D. Retinal detachment (arrowheads) in a 6-month-old *POMGnT1*-deficient mouse.

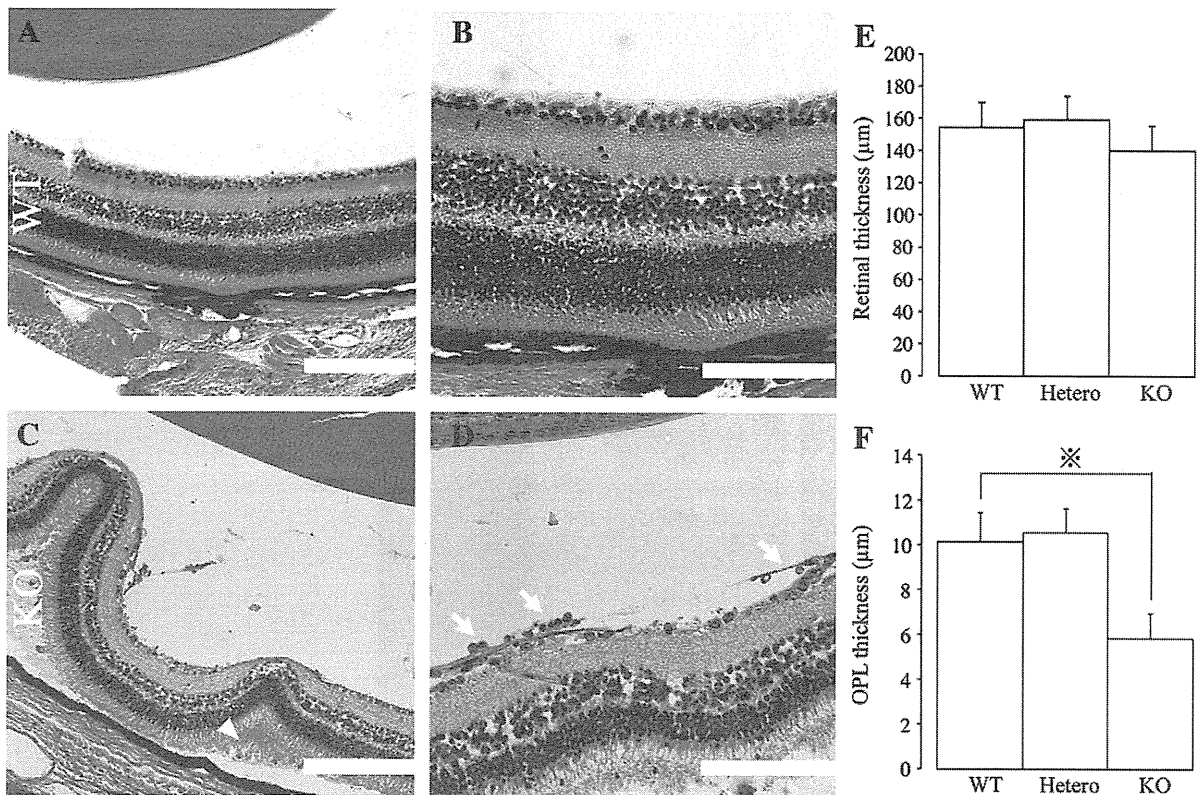


Fig. 2. Histological observations of the retina of wild-type and POMGnT1-deficient mice. A. and B. Sections of 15-week-old wild-type retinas stained with hematoxylin and eosin. C. and D. Sections of 15-week-old POMGnT1-deficient retinas stained with hematoxylin and eosin. In (C), focal retinal detachments can be seen in several regions. There are some connective tissue-like materials beneath the detached retina (arrowhead), indicating the retinal detachments are not embedding or sectioning artifacts. In (D), ectopic cells and vitreal fibroplasia can be seen on the ILM of POMGnT1-deficient retina (arrows). Scale bars represent 200 μm in A, C and 100 μm in B, D E and F. Quantification of the retinal thickness-measurements of wild-type, Heterozygous and Homozygous POMGnT1-deficient mice. Animals used for this study ranged from 18-week-old to 28-week-old. The average of each 5 animals is plotted. There was no significant difference in the whole retinal thickness (E), but significant thinning of the OPL was observed in POMGnT1-deficient mice compared to wild-type mice ($10.12 \pm 1.34 \mu\text{m}$ [SD] vs. $5.84 \pm 1.13 \mu\text{m}$; $P = 0.045$) (F).

more than a quadrant of the retina (Fig. 1D). By 12-months-of-age, 13 of 16 mutant eyes (81%) showed obvious retinal detachments.

Histological examination of 15-week-old mutant mice showed focal retinal detachments (Fig. 2C). Ectopic cells and vitreal fibroplasia were found on the inner limiting membrane (ILM; Fig. 2D) as was found in *Large^{vis}* mice (Lee et al., 2005). There were no significant difference in the whole retinal thickness, but significant thinning of the OPL was observed in POMGnT1-deficient mice compared to wild-type mice (Figs. 2E and F). This fibroplasia was immunopositive for glial fibrillary acidic protein (GFAP; Figs. 3C and D). Because GFAP expression is a reliable early marker of reactive gliosis of the astrocytes and Müller glial cells (Lewis and Fisher, 2003), an up-regulation of GFAP staining of the ILM and the radial immunoreactivity in the mutant mice indicated the development of reactive gliosis of the Müller cells. Quantitative analysis revealed that GFAP immunoreactivity was significantly elevated in the retina of POMGnT1-deficient mice (Fig. 3E). To confirm if elevated immunoreactivity of GFAP is truly associated with gliosis, we have also characterized the retina of POMGnT1-deficient mice using anti-vimentin antibody that is other cellular marker associated with gliosis. The vimentin immunoreactivity of POMGnT1-deficient mice along with ILM and radial morphology of Müller cells are also upregulated compared to that of wild-type mice (Figs. 4A and B). We have applied another cellular markers to characterize the different cell types in the anatomical regions. Immunoreactivity for both anti-syntaxin antibody and anti-PCK antibody, cellular markers for amacrine cells and bipolar cells, revealed no obvious differences between POMGnT1-deficient and wild-type mice (Figs. 4C–F). These data indicate that the up-regulation of GFAP and vimentin immuno-

reactivity is specifically associated with gliosis of Müller cells of the POMGnT1-deficient mice in the region.

Electroretinographic findings of POMGnT1-deficient mice

To examine the function of the retina of POMGnT1-deficient mice, ERGs were recorded from 4-month-old wild type and POMGnT1-deficient mice. The mixed rod-cone ERGs recorded from POMGnT1-deficient mice at higher stimulus intensities had a negative waveform with the amplitude of the b-wave smaller than that of the a-wave (Fig. 5A). Amplitudes of the a-wave and b-wave of mixed rod-cone ERGs obtained from POMGnT1-deficient mice are reduced significantly compared to wild-type mice (Figs. 5B and C). The amplitudes of the scotopic b-wave elicited by lower stimulus intensities were also reduced in POMGnT1-deficient mice (Fig. 5D). The amplitude of the b-wave of photopic ERGs of POMGnT1-deficient mice was also reduced and significantly smaller than that of wild-type mice (Fig. 5E).

Expression of alpha-DG and dystrophin in retina of POMGnT1-deficient mice

To confirm that the retina of POMGnT1-deficient mice completely lacked POMGnT1 enzyme activity, we used a monoclonal antibody, VIA4-1, that reacts against the sugar moiety of alpha-DG. Our findings showed that VIA4-1 immunoreactivity was present on the ILM, around blood vessels, and in the OPL of the retina of the wild type mice but was completely absent in the POMGnT1-deficient mice (Figs. 6A and B). It has been clearly shown that at the OPL there are three DMD gene products, Dp427 (or full length dystrophin), Dp260 and Dp140 and at

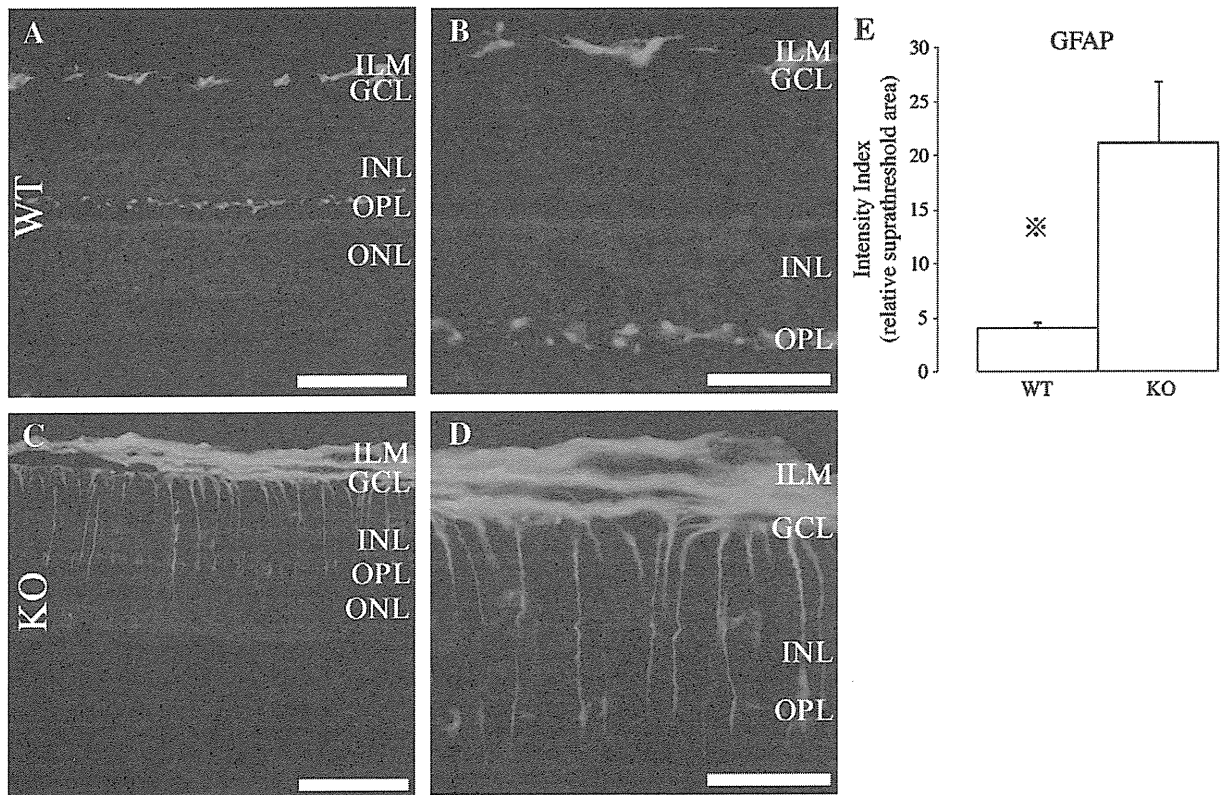


Fig. 3. GFAP staining of paraffin sections from wild-type and POMGnT1-deficient mice. A. and B. Sections of 18-week-old wild-type retinas with GFAP staining. C. and D. Sections of 18-week-old POMGnT1-deficient retinas. There was an up-regulation of GFAP staining in the ILM. Scale bars represent 100 μ m in A, C and 50 μ m in B, D and E. Quantification of GFAP immunoreactivity in paraffin sections from wild-type and POMGnT1-deficient mice. Animals used for this study ranged from 18-week-old to 28-week-old. The average of each 3 animals is plotted. Intensity Index for GFAP immunoreactivity was significantly elevated in the retina of POMGnT1-deficient mice compared to wild-type mice (3.90 ± 0.54 [SD] vs. 20.61 ± 5.65 ; $P = 0.003$).

the Müller cells only Dp71 is found (Daloz et al., 2003 and Fort et al., 2008). The expression of Dp71 in the ILM and around retinal blood vessels of POMGnT1-deficient mice was severely reduced (Fig. 6D). The expression of Dp427, Dp260, Dp140 were also reduced in the OPL of the mutant mice (Fig. 6D).

Glial proliferation closely associated with ER-TR7-positive fibrous tissue around abnormal retinal vessels in POMGnT1-deficient mice

Two mouse models with aberrant glycosylation of alpha-DG have been reported to have reactive gliosis with an up-regulation of GFAP expression in the retina and the brain. One of these is the *Large^{vlis}* mice, which has a disorganization of astrocytic processes in the retina (Lee et al., 2005). The second mutant is the POMGnT1-disrupted mouse, which has reactive gliosis in the cerebral cortex (Yang et al., 2007). To further characterize the glial proliferation and associated vascular abnormalities in the retina of our POMGnT1-deficient mice, we examined flat mounts of the retina of 4-month-old wild type and POMGnT1-deficient mice.

In flat mounts of POMGnT1-deficient mice retina, the GFAP staining of astrocytes was highly irregular especially around the retinal vasculature (Figs. 7E and K). Retinal vascular staining derived from perfusion of FITC-dextran showed disorganization of the normal pattern of the vascular networks (Figs. 7D and J). Double staining for GFAP and FITC-dextran showed that abnormal retinal vasculature was highly co-localized with the irregular astrocytic processes (Figs. 7F and L). Quantitative analysis for GFAP immunoreactivity and vascularization stained by FITC dextran perfusion showed significant elevation of intensity index in both central and peripheral retina of POMGnT1-deficient mice compared to wild-type mice (Fig. 8).

In POMGnT1-deficient mice, it was also reported that most of the GFAP-positive reactive astrocytes in the brain were in close contact with ectopic fibroblasts, suggesting that they were induced by the fibroblasts (Yang et al., 2007). To confirm that our POMGnT1-deficient mice also showed fibrosis associated with the GFAP-positive reactive astrocytes in the retina, we examined flat mounts of 4-month-old wild type and POMGnT1-deficient mice using the ER-TR7 antibody. Although the antigen of the ER-TR7 antibody has not been fully characterized, it is known to detect an antigen present in and produced by reticular fibroblasts. Reticular fibers are synthesized by a family of collagen proteins, and the fibers are made by reticular fibroblasts.

In the flat mount preparations, ER-TR7-positive fibrous tissue was found closely associated with GFAP-positive reactive astrocytes especially around the optic nerve head (Figs. 9D–F). An up-regulation of ER-TR7-positive fibrous tissue was also found in the peripheral retina associated with the irregular retinal vasculature (Figs. 9J–L).

Discussion

Patients with MEB show a variety of ocular abnormalities, and at least six cases with retinal detachment have been reported (Cormand et al., 2001; Matsumoto et al., 2005; Godfrey et al., 2007; Demir et al., 2009). Although an involvement of the retina has been frequently described in MEB patients, many patients without any retinal abnormalities have also been reported (Mercuri et al., 2009). A broader phenotypic spectrum was reported for MEB disease worldwide, and no consistent genotype–phenotype correlation has been established (Hehr et al., 2007). Thus, Finnish patients homozygous for the founder mutation showed a wide variation in their phenotype (Diesen et al., 2004).

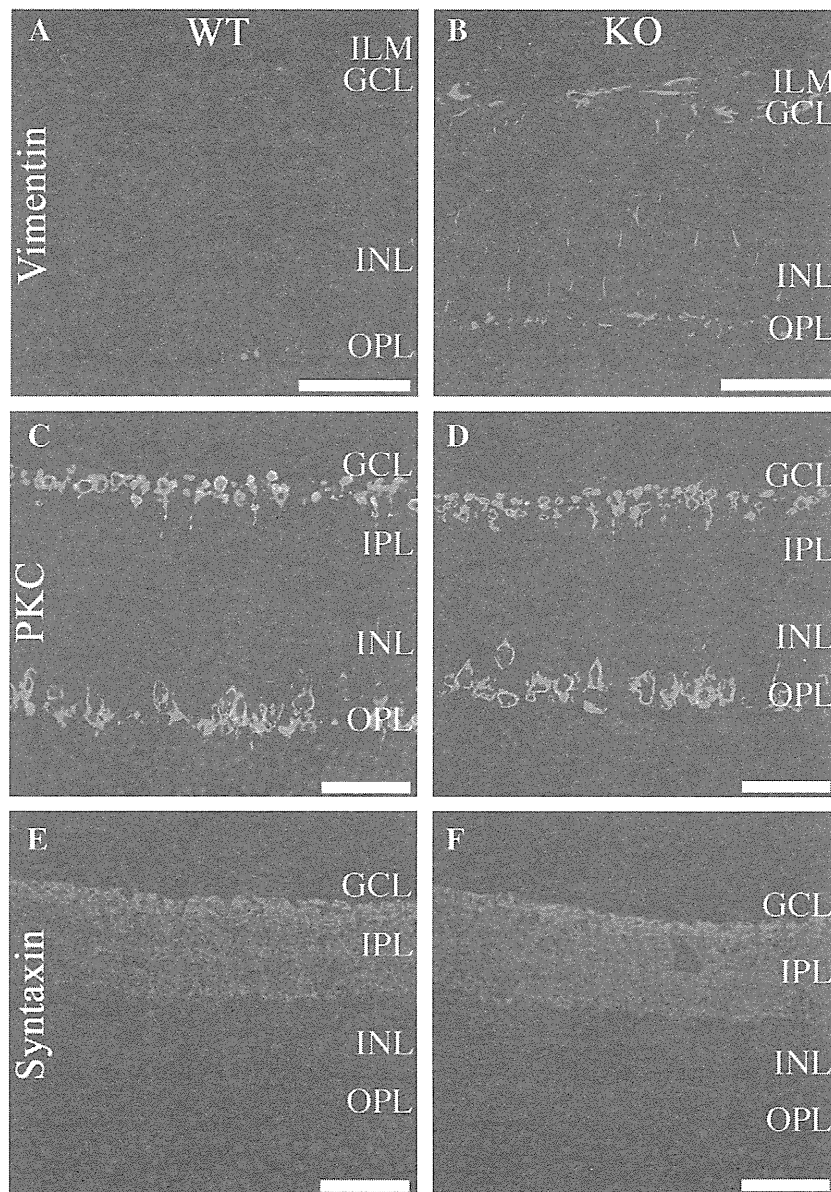


Fig. 4. Immunohistochemical observations of several markers for different cell types of the regions from 18-week-old wild-type and 20-week-old POMGnT1-deficient mice. A. and B. Sections of retina labeled with anti-vimentin antibody. The vimentin immunoreactivity of POMGnT1-deficient mice along with ILM and radial morphology of Müller cells were upregulated compared to that of wild-type mice. C. and D. Sections of retina labeled with anti-PKC antibody for bipolar cells. There were no significant differences between the retina of wild-type and POMGnT1-deficient mice. E. and F. Sections of retina labeled with anti-Syntaxin antibody for amacrine cells. There were no significant differences between the retina of wild-type and POMGnT1-deficient mice. Scale bars represent 50 μ m in A–F.

Two mouse models with mutations of the *POMGnT1* gene have been reported including our model (Liu et al., 2006 and Hu et al., 2010; Miyagoe-Suzuki et al., 2009). These two mouse models have different phenotypes and different location of the *POMGnT1* gene mutation. Our model was produced by standard gene targeting techniques with disruption of exon 18, while the other model was generated by gene trapping with a retroviral vector inserted into exon 2 of the *POMGnT1* gene. Our model has a milder muscle phenotype and a lower survival rate than the other model, but had frequent retinal detachment which was not described in the other model. Homozygous mutants of our mouse model are sterile, and homozygous mutants are obtained by heterozygote matings. However, the homozygous offspring have a very low survival rate (Miyagoe-Suzuki et al., 2009).

A spectrum of retinal abnormalities was observed in our POMGnT1-deficient mice, although all of these mice had the same *POMGnT1* gene mutation. These findings are consistent with earlier

hypotheses that factors other than the activity of *POMGnT1* gene, e.g., environmental factors, play a role in determining the severity of the mutation (Diesen et al., 2004; Matsumoto et al., 2005).

Abnormal ERGs are found in patients and mice with a mutation in the DGC component (Pillers et al., 1993; Pihko et al., 1995; Kameya et al., 1997). These findings suggest an involvement of the DGC localized in the OPL for signal transduction at the ribbon synapse of photoreceptor terminals. Mice with targeted disruption with pikachurin gene support this hypothesis. The reduced ERG b-waves in pikachurin-deficient mice suggest an involvement of DGC and pikachurin in retinal signal transduction at the ribbon synapses of photoreceptors (Sato et al., 2008). Recently, mice with a conditional deletion of dystroglycan in the CNS were generated by Satz et al. These mice showed that an inactivation of the glial specific dystroglycan located in the glial endfeet of Müller cells and perivascular astrocytes was sufficient to reduce the amplitude of the ERG b-wave (Satz et al., 2009).

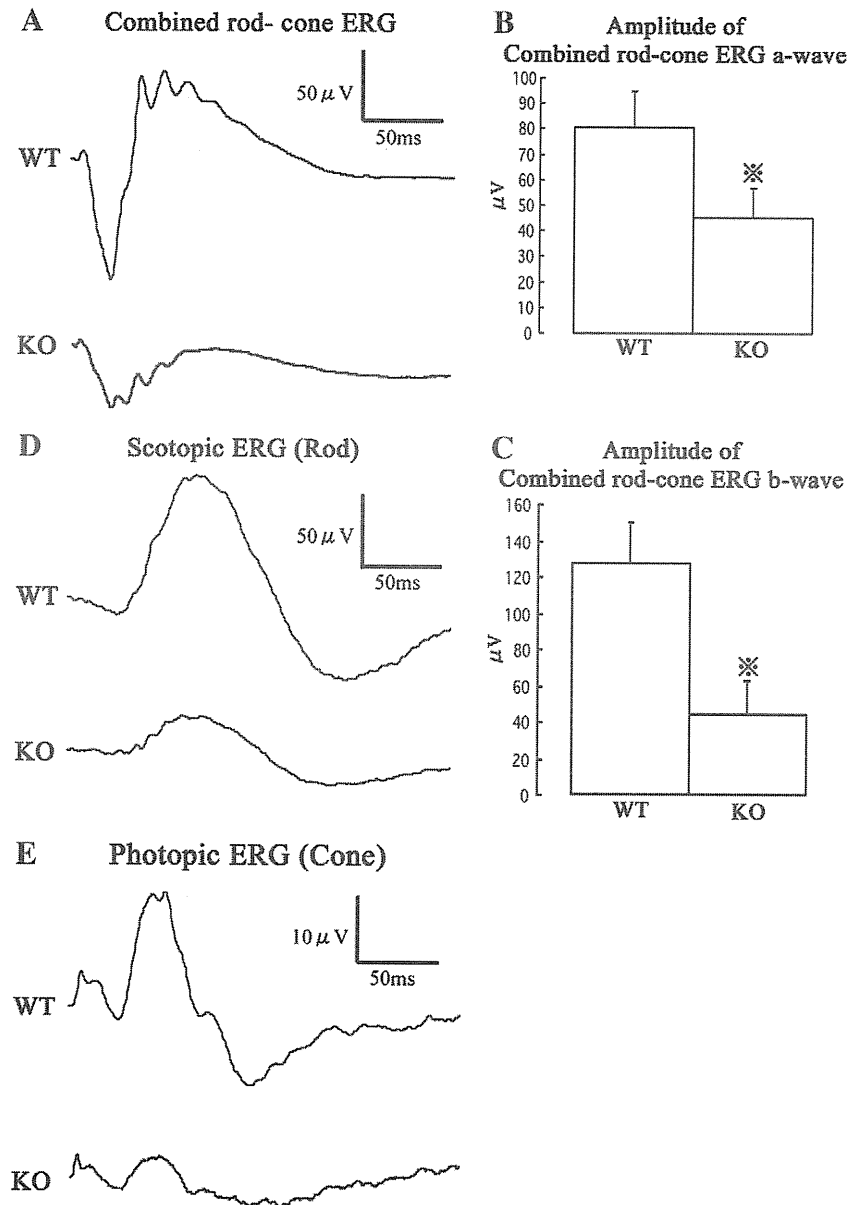


Fig. 5. Electrorretinograms of wild-type and POMGnT1-deficient mice. Animals used for this study ranged from 11-week-old to 19-week-old. A. Combined rod-cone ERGs obtained from POMGnT1-deficient mouse showing negative-type ERG with decreased amplitude of a-wave and b-wave. B. and C. Amplitudes of the a-wave and b-wave of combined rod-cone ERGs obtained from POMGnT1-deficient mice are reduced significantly compared to wild-type mice. The average of each 3 animals is plotted. D. and E. Amplitudes of the b-wave of scotopic and photopic ERGs obtained from POMGnT1-deficient mice are also decreased compared to wild-type mice.

The abnormal ERGs of POMGnT1-deficient mice could be explained by several mechanisms. They could arise from an inactivation of glial specific alpha-DG, or disturbed Pikachurin-DG interaction at the ribbon synapse, or dysfunction of retina caused by vascular network abnormalities, or the retinal detachments.

POMGnT1-deficient mice showed decreased expression of dystrophin in the ILM similar to that observed in the mice with conditional deletion of dystroglycan in the CNS, suggesting inactivation or dysfunction of alpha-DG caused by hypoglycosylation.

Pikachurin is necessary for the apposition of presynaptic and postsynaptic terminals in the photoreceptor ribbon synapses because Pikachurin is an extracellular ligand of alpha-dystroglycan at ribbon synapses (Sato et al., 2008). A recent study using the same POMGnT1-deficient model clearly showed that the degree of pikachurin immunoreactivity in the ribbon synapse of the mutant mice is reduced (Kanagawa et al., 2010). Because a proper localization of pikachurin at the ribbon synapse supported by functionally mature DG plays

important roles in the physiology of the retina, reduced expression of pikachurin in the mutant mice caused by disturbed pikachurin-DG interaction could be one of the cause of abnormal ERG of POMGnT1-deficient mice.

The vascular networks in the mutant retina were grossly disorganized associated with GFAP-positive irregular astrocytic processes compared to that of wild-type mice. The dysfunction of the mutant retina caused by the disorganization of retinal vascular network might be one of the causes of abnormal ERGs of mutant mice.

We have obtained the ERG data from the mice without gross retinal detachment, because retinal detachment is generally known to cause abnormal ERGs. However, we cannot rule out the possibility that these mice had shallow and focal retinal detachment associated with sheathed retinal vessels caused by the reactive gliosis.

In the retina, reactive gliosis can result from retinal injury and disease, including retinal trauma, choroidal neovascularization, retinal detachment, and diabetic retinopathy (MacLaren, 1996; Caicedo et al.,

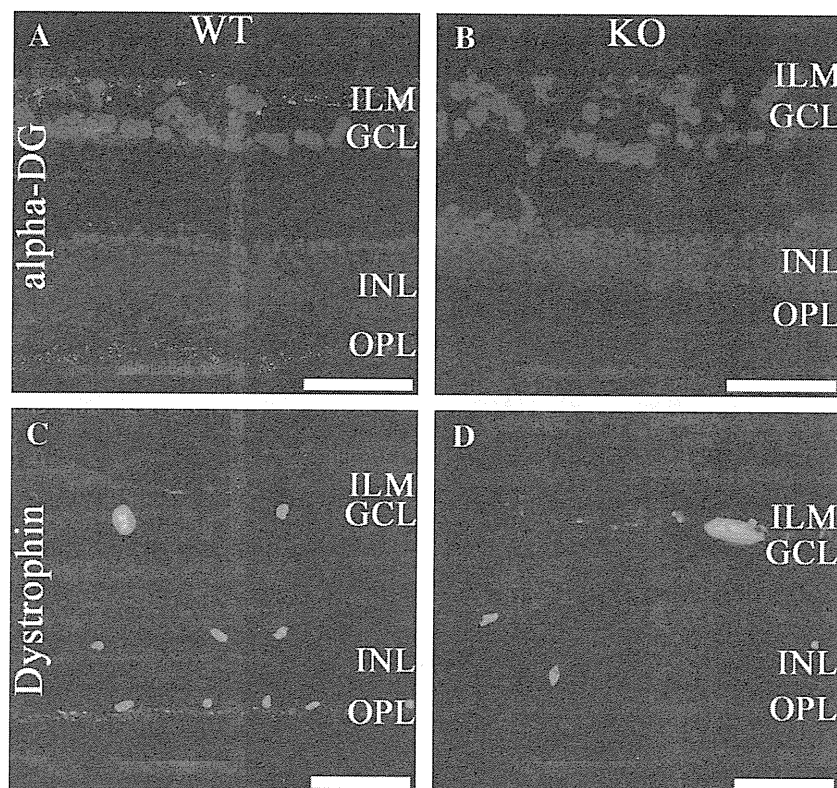


Fig. 6. Immunohistochemical observations of the dystrophin–glycoprotein complex in the retina from 18-week-old wild-type and 20-week-old POMGnT1-deficient mice. **A.** Sections of wild-type retina labeled with the VIA4-1 antibody for alpha-dystroglycan. VIA4-1 staining was found in ILM, around blood vessels, and in the OPL. **B.** VIA4-1 immunoreactivity was completely absent in POMGnT1-deficient retina. **C.** Sections of wild-type retinas labeled with the MAB1694 antibody for Dystrophin. Expression of Dystrophin can be seen in ILM, around blood vessels, and in the OPL. **D.** In the retina of POMGnT1-deficient mice, expression of Dystrophin was reduced in ILM, around the blood vessels and OPL. Scale bars represent 50 μm in A–D.

2005; Lewis et al., 1995; Mizutani et al., 1998). Secondary complications induced by the reactive gliosis of the Müller cells and astrocytes are the development of fibrosis and proliferative vitreoretinopathy (PVR; Fisher and Lewis, 2003). The POMGnT1-deficient mice showed highly reactive gliosis with strong up-regulation of GFAP expression.

Flat mount preparations of the mutant mice also showed connective tissue-like ER-TR7-positive fibrosis. The high incidence of retinal detachments in POMGnT1-deficient mice may be caused by the PVR preceding the reactive gliosis and reticular fibrosis in the perivascular astrocytes and Müller cells. In POMGnT1-deficient mice, it was shown that repetitive injury caused more fibrosis and fatty infiltration in the tibialis anterior muscles (Miyagoe-Suzuki et al., 2009). Reactive gliosis with increased numbers of fibroblasts closely associated with capillaries in the cerebral cortex has been reported in POMGnT1-deficient mice (Yang et al., 2007). *Large^{vis}* mice with disruption of glycosyltransferase have abnormal retinal vessels with highly irregular GFAP staining similar to those observed in our mice (Lee et al., 2005). Our mutant mice also had ER-TR7-positive fibrosis associated with reactive astrocytes around both the optic nerve head and peripheral retina. These findings suggest that aberrant glycosylation of alpha-DG can cause fibroblast proliferation in the muscle, eye, and brain of these mice, and also reactive gliosis in the eye and brain.

On the other hand, mice with a complete loss of dystroglycan from the glial endfeet did not have abnormal retinal vasculature or gliosis (Satz et al., 2009). These results suggest that hypoglycosylation or incomplete glycosylation of alpha-DG rather than the absence of alpha-DG may play a role in reactive gliosis of perivascular astrocytes in the retina.

In conclusion, our findings indicate that POMGnT1-deficient mice may be a good model of human MEB. The reactive gliosis and reticular fibrosis in the perivascular astrocytes and Müller glial cells caused by

hypoglycosylation or incomplete glycosylation of alpha-DG may be associated with the mechanisms of retinal dysplasia, abnormal ERG and retinal detachment in human MEB. The phenotypic variability of the mutant mice may be useful to determine other factors than POMGnT1-deficiency in determining the severity of human MEB.

Experimental methods

Experimental animals

The generation of POMGnT1-deficient mice on C57BL/6 background was described in detail by Miyagoe-Suzuki et al. (2009). For our study, normal C57BL/6J mice were used as wild type control and were purchased from CLEA Japan, Inc. The procedures used in these experiments were approved by the Animal Care and Use Committee of the Nippon Medical School and conformed to the ARVO statement for the use of animals in ophthalmic and vision research.

Clinical examination of retina

The pupils of the mice were dilated with tropicamide and phenylephrine hydrochloride for indirect ophthalmoscopy with a 90 diopter aspheric lens. Fundus photographs were taken with a Kowa GENESIS-D fundus camera (Kowa Co., Japan) for small animals using a 90 diopter aspheric lens.

Histology and immunohistochemistry

Eyes from POMGnT1-deficient and C57BL/6J mice were enucleated and fixed in SuperFix (Kurabo, Osaka, Japan) overnight. They were then embedded in paraffin, and 7 μm thickness sections were stained